

Polarization Analysis of Thermal-Neutron Scattering*

R. M. MOON, T. RISTE,[†] AND W. C. KOEHLER

Solid State Division, Oak Ridge National Laboratory, Oak Ridge, Tennessee 37830

(Received 30 December 1968)

A triple-axis neutron spectrometer with polarization-sensitive crystals on both the first and third axes is described. The calculation of polarized-neutron scattering cross sections is presented in a form particularly suited to apply to this instrument. Experimental results on nuclear incoherent scattering, paramagnetic scattering, Bragg scattering, and spin-wave scattering are presented to illustrate the possible applications of neutron-polarization analysis.

I. INTRODUCTION

WE have added a new dimension to measurements of thermal-neutron scattering by constructing, at the Oak Ridge High-Flux Isotope Reactor, a triple-axis spectrometer with polarization-sensitive crystals on both the first and third axes. With this instrument the distribution of scattered neutrons from an initially monochromatic, polarized beam is measured as a function of angle, energy, and spin. The usual polarized-beam instrument is a two-axis diffractometer in which the measured cross section involves integration over the final energy and spin distributions. Information is lost in these integrations. We are able to measure cross sections for scattering from an initial state of specified momentum and spin to a final state of specified momentum and spin. In this paper we present a calculation of the appropriate cross sections and a series of experiments designed to explore the capabilities of this instrument and to demonstrate various applications of neutron-polarization analysis.

Because our approach to the calculation of polarized-neutron cross sections is strongly influenced by the capabilities of this instrument, we give here an idealized, brief description of its operation. The sample is maintained in a magnetic field which defines the direction of polarization for both the incident and scattered neutrons. The polarizing and analyzing crystals may be considered as devices which have zero reflectivity for (−) spin neutrons. Devices for reversing the polarization (flippers) are mounted before and after the sample. With both flippers off, the beam incident on the sample is in the (+) spin state and only those neutrons which are scattered without change of spin will be reflected by the analyzer. We thus measure a (++) cross section. With the first flipper on, the incident beam is in the (−) spin state but the analyzer will reflect only (+) neutrons, so that in this case we measure a spin-flip (−+) cross section. Similarly, with the second flipper on, we measure the (+−) cross section, and with both flippers on, we measure the (−−) cross section. It is thus natural to think in terms of these four partial cross sections and to talk of spin-flip scattering (+− and −+) and non-spin-flip

scattering (++ and −−). The theoretical quantities of greatest interest are the partial cross sections.

This is a different language than is customarily used by theoreticians in describing the scattering of polarized neutrons. The total cross section (summed over final spin states) and the final polarization are calculated as a function of the initial polarization. The polarization equation is a vector relationship giving the magnitude and direction of the final polarization. We measure only the component of the final polarization along the direction of the initial polarization. This remark is somewhat misleading, as is the title of this paper, because we do not measure polarization at all. Perhaps a more descriptive phrase might be “neutron-spin spectroscopy.” We measure cross sections connecting two neutron-spin states, from which the final polarization may be deduced if desired. Frequently, the final polarization is not particularly interesting.

In Sec. II, theoretical expressions for these cross sections are derived, and the apparatus is described in Sec. III. In the remaining sections, the general theory is specialized to particular interesting cases and illustrative experimental results are presented. Emphasis is placed on understanding experimental results in terms of the basic interactions between atoms and neutrons. These results include experiments on nuclear incoherent scattering, paramagnetic scattering, Bragg scattering, and magnon scattering from both ferromagnets and antiferromagnets. We believe the technique has important applications in a wide variety of problems.

II. THEORY

The fundamentals of the theory of polarized-neutron scattering were first presented by Halpern and Johnson.¹ More recently the theory has been developed by Maleev,^{2,3} by Sáenz,⁴ by Izyumov,^{5,6} by Marshall,⁷ by

¹ O. Halpern and M. R. Johnson, *Phys. Rev.* **55**, 898 (1939).

² S. V. Maleev, *Zh. Eksperim. i Teor. Fiz.* **33**, 129 (1958) [English transl.: *Soviet Phys.—JETP* **34**, 89 (1958)].

³ S. V. Maleev, *Zh. Eksperim. i Teor. Fiz.* **40**, 1224 (1961) [English transl.: *Soviet Phys.—JETP* **13**, 860 (1961)].

⁴ A. W. Sáenz, *Phys. Rev.* **119**, 1542 (1960).

⁵ Yu. A. Izyumov and S. V. Maleev, *Zh. Eksperim. i Teor. Fiz.* **41**, 1644 (1961) [English transl.: *Soviet Phys.—JETP* **14**, 1168 (1962)].

⁶ Yu. A. Izyumov, *Usp. Fiz. Nauk* **80**, 41 (1963) [English transl.: *Soviet Phys.—Usp.* **16**, 359 (1963)].

⁷ W. Marshall (unpublished).

* Research sponsored by the U. S. Atomic Energy Commission under contract with the Union Carbide Corporation.

[†] Guest scientist from Institutt for Atomenergi, Kjeller, Norway.

Blume,⁸⁻¹⁰ and by Steinsvoll.¹¹ In most of these papers the density-matrix formalism is used to derive expressions for the total cross section and polarization of the scattered beam as functions of the initial polarization. From these expressions it is possible to obtain the four partial cross sections in which we are interested. However, it is more instructive to obtain these cross sections directly, without going through the spin-density formalism. This makes the calculation less elegant, but much more transparent. The various polarization effects are most easily understood in terms of the atomic scattering amplitudes connecting the initial and final neutron-spin states. We make one important restriction at the outset: The final polarization is always to be analyzed in the direction of the initial polarization, in accordance with our experimental arrangement. This makes the calculation slightly less general, but the general case would be extremely difficult to examine experimentally. Classically, in a uniform field directed along the initial polarization, a scattered neutron with a general spin direction will begin to precess about the field direction, so it is only the component along the field which we observe. To measure a polarization not in the direction of the incident polarization would require a magnetic field which changes direction precisely at the location of the scattering center.

In Marshall's⁷ notation, the cross section for a scattering process in which the neutron wave vector changes from \mathbf{k} to \mathbf{k}' and its spin changes from state s to s' while the scattering system goes from state q to q' is

$$\frac{d^2\sigma^{ss'}}{d\Omega'dE'} = \sum_q P_q \sum_{q'} \frac{k'}{k} \left(\frac{m_0}{2\pi\hbar^2} \right)^2 \times \left| \left\langle s'q' \left| \int d\mathbf{r} e^{i\mathbf{K}\cdot\mathbf{r}} V(\mathbf{r}) \right| sq \right\rangle \right|^2 \times \delta \left(\frac{\hbar^2}{2m_0} (k'^2 - k^2) + E_{q'} - E_q \right), \quad (1)$$

where P_q is the probability that the system is in the initial state q and $\mathbf{K} = \mathbf{k} - \mathbf{k}'$. This is the familiar Born approximation with the δ function inserted to provide conservation of energy. Using the Halpern-Johnson¹ results for the interaction potential $V(\mathbf{r})$ and transforming the integral into a sum over atomic sites, we obtain

$$\frac{d^2\sigma^{ss'}}{d\Omega'dE'} = \sum_q P_q \sum_{q'} \frac{k'}{k} \left| \left\langle q' \left| \sum_i e^{i\mathbf{K}\cdot\mathbf{r}_i} U_i^{ss'} \right| q \right\rangle \right|^2 \times \delta(\Delta E_n + \Delta E_q), \quad (2)$$

⁸ M. Blume, Phys. Rev. **130**, 1670 (1963).

⁹ M. Blume, Phys. Rev. **133**, A1366 (1964).

¹⁰ R. I. Schermer and M. Blume, Phys. Rev. **166**, 554 (1968).

¹¹ O. Steinsvoll, Kjeller Report No. KR-65, 1963 (unpublished).

where

$$U_i^{ss'} = \langle s' | (b_i - p_i \mathbf{S}_{1i} \cdot \boldsymbol{\sigma} + B_i \mathbf{I}_i \cdot \boldsymbol{\sigma}) | s \rangle. \quad (3)$$

The quantities $U_i^{ss'}$ are seen to be atomic scattering amplitudes describing a process in which the neutron goes from spin state s to s' . In Eq. (3), b_i is the nuclear coherent scattering amplitude,¹² p is the magnetic amplitude,

$$p = (\gamma e^2 / 2mc^2) g S f(\mathbf{K}), \quad (4)$$

\mathbf{S}_1 is the negative of the Halpern \mathbf{q} vector defined in terms of the atomic-spin operator \mathbf{S} ,

$$\mathbf{S}_1 = \hat{\mathbf{S}} - (\hat{\mathbf{S}} \cdot \hat{\mathbf{K}}) \hat{\mathbf{K}}, \quad (5)$$

$\boldsymbol{\sigma}$ is the neutron-spin operator,¹³ \mathbf{I} is the nuclear-spin operator, and B is the spin-dependent nuclear amplitude.¹² In Eq. (4), γ is the magnitude of the neutron moment in nuclear magnetons (1.913), gS is the atomic moment in Bohr magnetons, and $f(\mathbf{K})$ is the normalized magnetic form factor. This is the Fourier inversion of the spin density if there is no orbital moment; otherwise $f(\mathbf{K})$ is a combination of spin and orbital form factors. For rare-earth ions g is the Landé factor and S should be replaced by the total angular momentum operator J . We are assuming that the moment distribution associated with a single atomic site is collinear,¹⁴ although there may be changes from site to site. We prefer the notation \mathbf{S}_1 , introduced by de Gennes,¹⁵ rather than the \mathbf{q} of Halpern and Johnson, as a reminder that only the atomic-spin component which is perpendicular to \mathbf{K} is effective in scattering neutrons.

Using the properties of the Pauli-spin operators, the four amplitudes described by Eq. (3) are found to be

$$U^{++} = b - p S_{1z} + B I_z, \quad (6a)$$

$$U^{--} = b + p S_{1z} - B I_z, \quad (6b)$$

$$U^{+-} = -p(S_{1x} + iS_{1y}) + B(I_x + iI_y), \quad (6c)$$

$$U^{-+} = -p(S_{1x} - iS_{1y}) + B(I_x - iI_y). \quad (6d)$$

In these equations, z refers to the direction of the neutron polarization. In reading the literature it is very easy to become confused over the proper algebraic sign for the magnetic scattering term because of the several definitions of the magnetic interaction vector and because the neutron moment is opposite to the neutron spin. We have chosen to display all the signs explicitly, that is, p is a positive quantity, and \mathbf{S}_1 is the projection

¹² If the nucleus has amplitude b^+ for the state $I + \frac{1}{2}$ and b^- for the state $I - \frac{1}{2}$, then

$$b = \frac{b^+(I+1) + b^-}{2I+1}$$

and

$$B = \frac{b^+ - b^-}{2I+1}.$$

¹³ If the neutron-spin states are designated as $(+)$ and $(-)$, then $\sigma_x(\pm) = \pm(\pm)$, $\sigma_y(\pm) = (\mp)$, and $\sigma_z(\pm) = \pm i(\mp)$. The factor $\frac{1}{2}\hbar$ has been absorbed in the definitions of p and B .

¹⁴ Evidence for the validity of this assumption in hexagonal Co will be presented in a future publication (see Ref. 21).

¹⁵ P.-G. de Gennes, in *Magnetism*, edited by G. T. Rado and H. Suhl (Academic Press Inc., New York, 1963), Vol. III, p. 115.

of the unit angular momentum vector onto the plane perpendicular to the scattering vector. The minus sign in Eq. (6a) means that in the production of a polarized beam by reflection off a Co crystal, the neutron-spin polarization is opposite to the Co spin, or parallel to the Co moment and to the applied field. Because Eq. (6) follows directly from Eq. (3) using only the Pauli-spin matrices, and because the form of the interaction as expressed in Eq. (3) is the same for orbital moment and spin moment, the various polarization effects to be discussed in terms of these amplitude equations apply regardless of the source of the atomic moment.

It is useful to pause at this point and examine Eq. (6). We see that coherent nuclear scattering is always non-spin-flip scattering ($++$ and $--$). Because isotopic disorder scattering results from a randomness in b_i , it is also non-spin-flip. The magnetic and nuclear-spin scattering is non-spin-flip if the effective spin components are along the neutron-polarization direction, and the scattering is spin-flip ($+-$ and $-+$) if the effective spin components are perpendicular to the polarization direction. For magnetic scattering it is only those spin components which are perpendicular to the scattering vector [see Eq. (5)] which are effective in neutron scattering. This brings us to an important special case. *If the neutron polarization is along the scattering vector ($S_{1z}=0$), then all magnetic scattering is spin-flip scattering.* This statement is true for all types of scattering: incoherent, coherent, elastic, or inelastic. Here is a very useful tool for separating magnetic from nuclear scattering.

Many interesting cases can be analyzed just by inspection of the amplitude equations (6). Because we will not consider in any detail the effects of nuclear polarization, we give here a brief example of the value of the amplitude equations by analyzing a special case with polarized nuclei. We assume a monoisotopic element with complete nuclear polarization in the $(+)$ direction and zero atomic moment. All the nuclei will have $I_z=I$, so the $(++)$ scattering will be completely coherent with an effective coherent amplitude of $b+BI$. If the incident beam is polarized in the $(-)$ direction, the coherent amplitude becomes $b-BI$. The incoherent scattering will be spin-flip scattering from the random distribution of x and y components of the nuclear spin. We note that the spin-flip amplitudes have the form of step-up and step-down angular momentum operators. For the fully polarized state, the step-up operator has no nonvanishing matrix elements, and the step-down operator has one nonvanishing matrix element of value $\sqrt{2I}$. We conclude that the incoherent scattering cross sections per atom are

$$\frac{d\sigma^{+-}}{d\Omega}=0, \quad \frac{d\sigma^{-+}}{d\Omega}=2IB^2.$$

Using the definitions of b and B ,¹² these results are

easily shown to be identical to those obtained by Schermer and Blume.¹⁰

To simplify the remaining discussion let us replace the magnetic and nuclear-spin operators by a single vector

$$\mathbf{A} = -\rho\mathbf{S}_1 + B\mathbf{I}, \quad (7)$$

and introduce the notation

$$\tilde{b}_i = \langle q' | b_i | q \rangle, \quad (8)$$

$$\tilde{\mathbf{A}}_{i\alpha} = \langle q' | \mathbf{A}_{i\alpha} | q \rangle, \quad (9)$$

$$W^{ss'} = |\langle q' | \sum_i e^{i\mathbf{K}\cdot\mathbf{r}_i} U_i^{ss'} | q \rangle|^2. \quad (10)$$

Equation (2) may now be written

$$\frac{d^2\sigma^{ss'}}{d\Omega'dE'} = \sum_q P_q \sum_{q'} \frac{k'}{k} W^{ss'} \delta(\Delta E_n + \Delta E_q). \quad (11)$$

Note that the symbols $W^{ss'}$, \tilde{b} , and $\tilde{\mathbf{A}}$ should really bear subscripts q' and q , which we are not showing. Expanding the double sum in Eq. (10), we find that

$$W^{\pm\pm} = \sum_{ij} e^{i\mathbf{K}\cdot(\mathbf{r}_i-\mathbf{r}_j)} (\tilde{b}_i\tilde{b}_j^* \pm \tilde{b}_i\tilde{\mathbf{A}}_{jz}^* \pm \tilde{\mathbf{A}}_{iz}\tilde{b}_j^* + \tilde{\mathbf{A}}_{iz}\tilde{\mathbf{A}}_{jz}^*), \quad (12a)$$

$$W^{\pm\mp} = \sum_{ij} e^{i\mathbf{K}\cdot(\mathbf{r}_i-\mathbf{r}_j)} [\tilde{\mathbf{A}}_{xi}\tilde{\mathbf{A}}_{xj}^* + \tilde{\mathbf{A}}_{yi}\tilde{\mathbf{A}}_{yj}^* \mp i\hat{z}\cdot(\tilde{\mathbf{A}}_i\times\tilde{\mathbf{A}}_j^*)], \quad (12b)$$

The partial cross sections are found by substituting (7)–(9) into (12) and then substituting the resulting expressions into (11). If the instrument described previously is working perfectly, the measured quantities are these partial cross sections.

It is also of interest to combine the partial cross sections to get expressions for the total cross section and polarization of the scattered beam. These expressions may then be compared with the density-matrix results. If n^+ and n^- are the probabilities of finding a neutron in the initial spin states, the total cross section is

$$\sigma = n^+(\sigma^{++} + \sigma^{+-}) + n^-(\sigma^{--} + \sigma^{-+}), \quad (13)$$

and the final polarization is

$$\sigma P_f = n^+\sigma^{++} + n^-\sigma^{-+} - n^-\sigma^{--} - n^+\sigma^{-+}, \quad (14)$$

where

$$\sigma^{ss'} = \frac{d^2\sigma^{ss'}}{d\Omega'dE'} \quad (15)$$

and

$$n^+ + n^- = 1. \quad (16)$$

The initial spin populations are given in terms of the initial polarization by

$$n^+ = \frac{1}{2}(1 + P_0) \quad (17)$$

and

$$n^- = \frac{1}{2}(1 - P_0). \quad (18)$$

Performing the indicated substitutions, we find that the cross section is

$$\begin{aligned} \frac{d^2\sigma}{d\Omega'dE'} = \sum_{qa'} P_q \frac{k'}{k} \left\{ \sum_{ij} e^{i\mathbf{K}\cdot(\mathbf{r}_i - \mathbf{r}_j)} [\tilde{b}_i \tilde{b}_j^* + \tilde{\mathbf{A}}_i \cdot \tilde{\mathbf{A}}_j^* \right. \\ \left. + \mathbf{P}_0 \cdot (\tilde{b}_i \tilde{\mathbf{A}}_j^* + \tilde{b}_j^* \tilde{\mathbf{A}}_i - i \tilde{\mathbf{A}}_i \times \tilde{\mathbf{A}}_j^*)] \right\} \\ \times \delta(\Delta E_n + \Delta E_q), \quad (19) \end{aligned}$$

where $\mathbf{P}_0 = P_0 \hat{z}$, and the polarization along \hat{z} is

$$\begin{aligned} P_f \frac{d^2\sigma}{d\Omega'dE'} = \sum_{qa'} P_q \frac{k'}{k} \left\{ \sum_{ij} e^{i\mathbf{K}\cdot(\mathbf{r}_i - \mathbf{r}_j)} [\hat{z} \cdot (\tilde{b}_i \tilde{\mathbf{A}}_j^* + \tilde{b}_j^* \tilde{\mathbf{A}}_i \right. \\ \left. + i \tilde{\mathbf{A}}_i \times \tilde{\mathbf{A}}_j^*) + P_0 (\tilde{b}_i \tilde{b}_j^* + \tilde{A}_{zi} \tilde{A}_{zj}^* - \tilde{A}_{xi} \tilde{A}_{xj}^* \right. \\ \left. - \tilde{A}_{yi} \tilde{A}_{yj}^*)] \right\} \delta(\Delta E_n + \Delta E_q). \quad (20) \end{aligned}$$

The cross section is identical to that obtained by the density-matrix formalism and needs no further discussion. The polarization can be obtained from the general expression (see Ref. 8) by taking the product $\hat{z} \cdot \mathbf{P}_f$. All the terms in the general \mathbf{P}_f are given by Eq. (20), except for those of type $(\mathbf{P}_0 \times \mathbf{A})\tilde{b}$, which rotate the polarization perpendicular to the incident polarization. We cannot observe such terms in our experimental arrangement. In Eq. (20) the first two terms are the familiar nuclear-magnetic interference terms which are commonly used in producing polarized beams. The next term is effective in producing polarization in magnon scattering and in elastic scattering from spiral structures. The physical content of these terms may be expressed by stating that to produce polarization there must be an axial vector built into the system—either as a ferromagnetic or spiral (static or dynamic) arrangement. This point of view has been emphasized by Izyumov and Maleev.⁵ The last four terms show again that the initial polarization is preserved in non-spin-dependent nuclear scattering and in scattering by spin components along the polarization direction, while transverse spin components reverse the polarization direction.

Equations (19) and (20) serve to point out the differences between the usual polarized-beam experiment (without analyzer), in which only the total cross section is measured, and the polarization analysis experiment, in which both the cross section and the final polarization may be obtained. The former experiment is limited to systems which have a polarization-dependent cross section (ferromagnets, spirals, and some antiferromagnets), while even a random collection of spins will produce changes in the polarization and such systems may be profitably investigated by the polarization analysis technique.

III. APPARATUS

The instrument is one of a pair of triple-axis, computer-controlled spectrometers¹⁶ installed at the High-Flux Isotope Reactor. The experimental arrangement is shown schematically in Fig. 1. A similar experiment has been proposed by Misenta.¹⁷ Co-Fe crystals mounted in the gap of a permanent magnet are used on the first and third axes for production of the polarized, monochromatic beam and for analysis of scattered neutrons in energy and spin. The sample is mounted in the gap of an electromagnet located on the table of the second axis. This electromagnet has a horizontal rotation axis

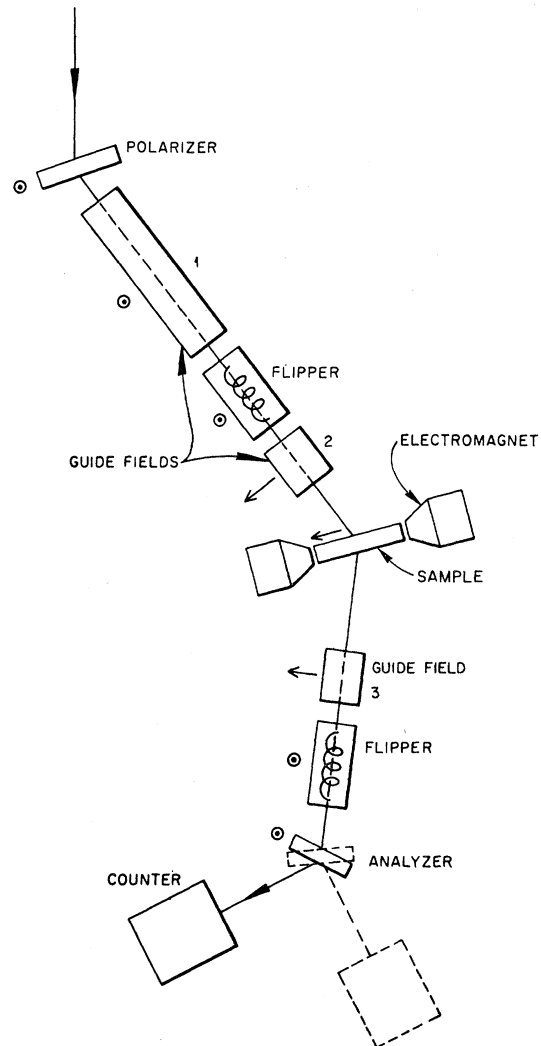


FIG. 1. Experimental arrangement. Arrows adjacent to the guide fields show the direction of the magnetic field sensed by the neutrons.

¹⁶ M. K. Wilkinson, H. G. Smith, W. C. Koehler, R. M. Nicklow, and R. M. Moon, in *Neutron Inelastic Scattering* (International Atomic Energy Agency, Vienna, 1968), Vol. II.

¹⁷ R. Misenta, Euratom Report Nos. EUR3291, 1967, and EUR3910, 1968 (unpublished).

so that the field is easily changed from vertical to horizontal. The guide fields 2 and 3 can also be rotated so that the neutrons can be brought into the field of the electromagnet in either a vertical or horizontal orientation. Radio-frequency coils with a vertical guide field are used as flipping devices. We have not yet used two coils simultaneously, as indicated in Fig. 1, but have moved a single coil from before to after the sample as experimental conditions dictate. With the sample field in the horizontal direction the neutron polarization follows the local guide field (shown by arrows in Fig. 1) through several adiabatic rotations. The first one occurs in the region between the first flipper and guide field 2 where there is a rotation of the polarization from vertical to horizontal. The second occurs as the neutrons enter the fringing field of the electromagnet so that at the sample position the neutrons are polarized in the direction of the central field of the electromagnet. Reversed rotations occur along the exit trajectory so that the polarization at the analyzing position is vertical. With the sample field in the vertical direction the neutron polarization remains vertical throughout. The four partial cross sections can be measured as outlined in the Introduction by proper manipulation of the flippers.

The over-all efficiency of the system can be measured by rotating the analyzing crystal into the incident beam and measuring the ratio of neutrons reflected by the analyzer with the flipper "off" and "on." This flipping ratio varies with wavelength and beam size between 60 and 120. The performance in the horizontal field configuration is nearly identical to that in the vertical field configuration. A flipping ratio of 100 implies that the beam polarization and flipping efficiency are both in the range 0.98–1.0. Corrections to account for instrumental imperfections can be calculated, but for many experiments the instrument is good enough so that these corrections are negligible.

IV. INCOHERENT SCATTERING

Isotopic Incoherent Scattering

As already noted, this type of scattering results from a random disorder in the nuclear amplitudes b_i and hence is entirely non-spin-flip scattering. Since the energy of the system is independent of the isotope distribution, we can write immediately that the cross section per atom is

$$\frac{d\sigma^{++}}{d\Omega} = \frac{d\sigma^{--}}{d\Omega} = \langle b^2 \rangle_{av} - \langle b \rangle_{av}^2 \quad (21)$$

and

$$\frac{d\sigma^{+-}}{d\Omega} = \frac{d\sigma^{-+}}{d\Omega} = 0. \quad (22)$$

An example of this type of scattering is shown in Fig. 2 for the case of Ni.

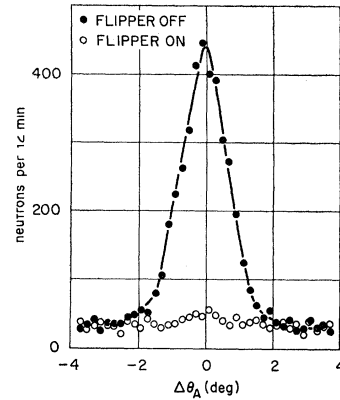


FIG. 2. Isotopic incoherent scattering from Ni. The data were obtained by rocking the analyzer through the elastic position with fixed scattering angle. The "flipper-off" data are proportional to the $(++)$ cross section and the "flipper-on" data are proportional to the $(-+)$ cross section.

Nuclear-Spin Incoherent Scattering

For the present we assume a nonmagnetic system with randomly oriented nuclear spins. The operator \mathbf{A} in (12) is then $B\mathbf{I}$. In performing the double sum, only terms of type $I_{ix}I_{ix}$, $I_{iy}I_{iy}$, and $I_{iz}I_{iz}$ will contribute because of the random orientation. Each of these terms is equal to $\frac{1}{3}I(I+1)$, so we conclude that the cross sections per atom are

$$\frac{d\sigma^{++}}{d\Omega} = \frac{d\sigma^{--}}{d\Omega} = \frac{1}{3}B^2I(I+1), \quad (23)$$

$$\frac{d\sigma^{+-}}{d\Omega} = \frac{d\sigma^{-+}}{d\Omega} = \frac{2}{3}B^2I(I+1). \quad (24)$$

We have assumed that the energy of the system is independent of the nuclear-spin orientation, so that the scattering is elastic. Note that the result is independent of the neutron-polarization direction. If the initial polarization is unity, the polarization in the scattered beam will be $-\frac{1}{3}$. This is a well-known theoretical result, but we believe that Fig. 3 represents the first experimental verification of this effect. The spin-flip $(-+)$ scattering from vanadium is seen to be twice as large as the non-spin-flip $(++)$ scattering and is independent of the neutron-polarization direction. We have also observed this effect in the quasi-elastic scattering from water and polyethylene.

This effect should have important applications wherever the separation of coherent and spin-incoherent nuclear scattering is a problem. Hydrogenous materials in general and liquids with large spin-incoherent cross sections are two obvious cases of interest. Note that the assumption that the energy of the system is independent of the nuclear-spin orientation is not true in many hydrogenous systems. It should also be noted that multiple scattering, as always, complicates the

interpretation of results. The final polarization of doubly scattered neutrons by random nuclear spins will be $+\frac{1}{9}P_0$.

Paramagnetic Scattering

Paramagnetic scattering is similar to the nuclear-spin scattering, except that only those atomic-spin components which are perpendicular to \hat{K} are effective in scattering neutrons. In the expressions for the scattering amplitudes [Eqs. (6)], if S_{1z} is zero ($\hat{K} \cdot \hat{P}_0 = 1$), the scattering will be entirely spin-flip. If S_{1z} is zero ($\hat{K} \cdot \hat{P}_0 = 0$), the scattering will consist of equal parts of spin-flip and non-spin-flip. We expect the final polarization to vary between 0 and $-P_0$, depending on the angle between \hat{P}_0 and \hat{K} . For the partial cross sections we obtain

$$\frac{d\sigma^{++}}{d\Omega} = \frac{d\sigma^{--}}{d\Omega} = \frac{1}{3} \left(\frac{\gamma e^2}{2mc^2} \right)^2 f^2 g^2 S(S+1) [1 - (\hat{P}_0 \cdot \hat{K})^2], \quad (25)$$

$$\frac{d\sigma^{+-}}{d\Omega} = \frac{d\sigma^{-+}}{d\Omega} = \frac{1}{3} \left(\frac{\gamma e^2}{2mc^2} \right)^2 f^2 g^2 S(S+1) [1 + (\hat{P}_0 \cdot \hat{K})^2], \quad (26)$$

and the final polarization is

$$P_f = -(\hat{P}_0 \cdot \hat{K})^2 P_0. \quad (27)$$

This expression for the polarization was first derived by Halpern and Johnson.¹ In writing down the above cross sections we have assumed a negligible energy transfer in the scattering. To illustrate these effects experimentally we have chosen MnF_2 , which should scatter neutrons with energy change small compared to our instrumental energy resolution. Figure 4 shows that the theoretical expectations are verified. The small peak in the "flipper-off" ($++$) data for the case $\hat{P}_0 \cdot \hat{K} = 1$ results from multiple Bragg scattering. The same effect is responsible for the slight difference in the two sets of data for the case $\hat{P}_0 \cdot \hat{K} = 0$.

It is in the area of paramagnetic scattering that we expect the technique of polarization analysis to have one of its most fruitful applications. The total cross

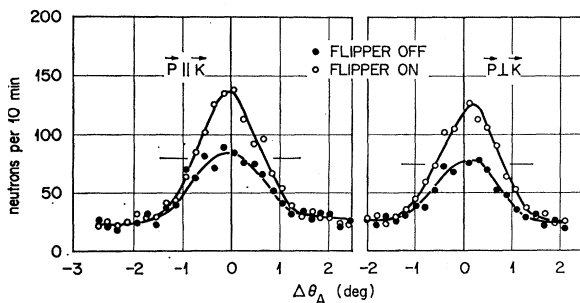


FIG. 3. Nuclear-spin incoherent scattering from vanadium. The data were obtained by rocking the analyzer through the elastic position with fixed scattering angle. The "flipper-off" data are proportional to the ($++$) cross section and the "flipper-on" data are proportional to the ($-+$) cross section.

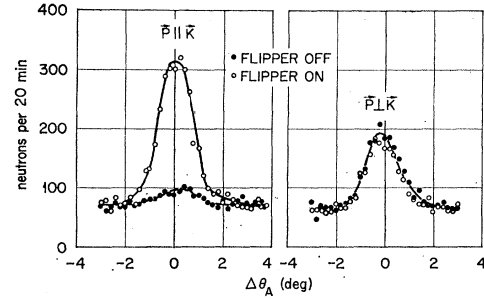


FIG. 4. Paramagnetic scattering from MnF_2 . The data were obtained by rocking the analyzer through the elastic position with fixed scattering angle. The "flipper-off" data are proportional to the ($++$) cross section and the "flipper-on" data are proportional to the ($-+$) cross section.

section is polarization-independent, so that nothing is gained by using a polarized beam without polarization analysis. With polarization analysis, many of the most difficult problems in analysis of paramagnetic scattering data are completely avoided. In the usual diffuse scattering experiment where the total cross section is measured, the following sources of scattering may be present: isotopic disorder, multiple Bragg, thermal diffuse (phonon), Bragg, nuclear spin incoherent, and paramagnetic. The problem of separating the paramagnetic scattering from the total scattering is formidable. However, the problem is enormously simplified by measuring the spin-flip scattering, since only the nuclear-spin and paramagnetic processes can contribute. For the case where $\hat{P}_0 \cdot \hat{K} = 1$ the spin-flip cross section is

$$\frac{d\sigma^{+-}}{d\Omega} = \frac{d\sigma^{-+}}{d\Omega} = \left(\frac{d\sigma}{d\Omega} \right)_{\text{para}} + \frac{2}{3} \left(\frac{d\sigma}{d\Omega} \right)_{\text{NS}}, \quad (28)$$

and for the case $\hat{P}_0 \cdot \hat{K} = 0$

$$\frac{d\sigma^{+-}}{d\Omega} = \frac{d\sigma^{-+}}{d\Omega} = \frac{1}{2} \left(\frac{d\sigma}{d\Omega} \right)_{\text{para}} + \frac{2}{3} \left(\frac{d\sigma}{d\Omega} \right)_{\text{NS}}, \quad (29)$$

where the cross sections on the right refer to the total paramagnetic and total nuclear-spin scattering. By measuring the spin-flip scattering for both of these cases, the paramagnetic and nuclear-spin scattering can be separated. If the nuclear spin is zero or if $(d\sigma/d\Omega)_{\text{NS}}$ is well known, only one case need be measured. As an added attraction, it should be mentioned that aluminum, which is commonly used in sample holders and cryostats for neutron experiments, has a negligible spin-flip cross section.

As an example of the usefulness of this technique, Fig. 5 shows the paramagnetic scattering pattern for MnF_2 . The data were collected in a step-scan mode of operation, similar to the usual powder technique, with the analyzer fixed to reflect elastically scattered neutrons. At each angle, counts were collected with the flipper off (non-spin-flip) and then with the flipper on (spin-flip). The two sets of data are shown separately,

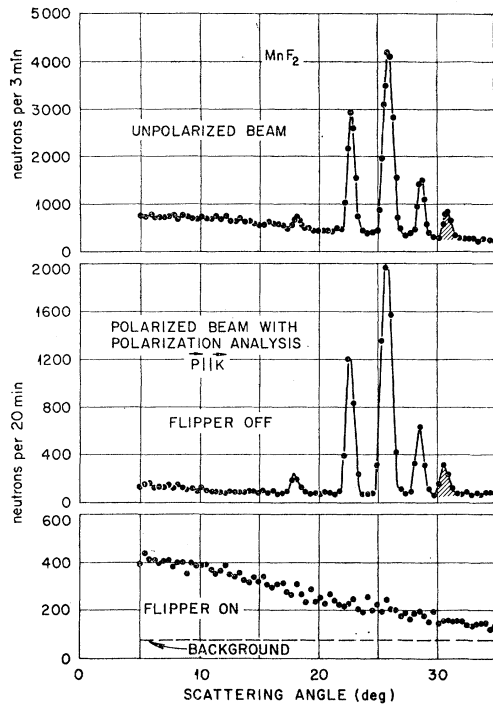


FIG. 5. MnF_2 powder pattern—separation of paramagnetic scattering through polarization analysis. No analyzer was used in the unpolarized-beam experiment. Note the loss of intensity in the polarization analysis experiment.

together with a conventional powder pattern (no analyzer) for which the counter collimation gave roughly equal angular resolution. Background data for the spin-flip scattering were collected by repeating the scan with the analyzer turned off the elastic position. Note that useful paramagnetic data are obtained even under the Bragg peaks. The wavelength was 1.07 \AA and the sample had a transmission of 0.82. Using the Bragg peaks in the non-spin-flip data to put the paramagnetic scattering on an absolute basis, the cross section shown in Fig. 6 was obtained. Slight corrections for instrumental imperfection were applied to the data obtained under the Bragg peaks and a small correction of 0.04 b/sr was applied to correct for nuclear-spin scattering. For comparison, the form factor obtained by Corliss *et al.*¹⁸ from Bragg scattering data on Mn^{++} was used to compute the paramagnetic cross section, normalized in the forward direction for $S = \frac{3}{2}$. The deviation at small angles has also been seen by Erickson¹⁹ and is probably related to magnetic short-range order.

As shown in Fig. 5, there is a loss in observed intensity of about a factor of 15 in going from the conventional two-axis arrangement to the triple axis with a cobalt analyzer at 1.07 \AA . If the cobalt monochromator were replaced with a good unpolarized-beam monochromator for the two-axis experiment, the intensity ratio would

¹⁸ L. M. Corliss, N. Elliott, and J. M. Hastings, *Phys. Rev.* **104**, 924 (1956).

¹⁹ R. A. Erickson, *Phys. Rev.* **90**, 779 (1953).

approach 100. The need for a high-flux reactor and development of high-reflectivity polarizing crystals is apparent for experiments involving incoherent scattering.

If we set aside the intensity problem, the study of magnetic impurities is an ideal area for application of the polarization analysis technique. Up to the present, it has been possible to study impurities only in ferromagnets with neutron scattering techniques. In this case the ability to control the direction of the atomic moments is exploited to separate the magnetic disorder scattering from other sources of scattering. With the polarization analysis technique, it should be possible to study paramagnetic impurities in a nonmagnetic matrix, to study impurities in antiferromagnets, and to extend the study of ferromagnetic systems to temperatures above the Curie point.

V. BRAGG SCATTERING

The interesting applications of polarization analysis in the field of Bragg scattering can be most easily seen by inspection of the amplitude equations (6). We restrict the discussion to systems with zero nuclear polarization so that we can neglect all terms involving the nuclear moment in discussing the Bragg scattering. The nuclear peaks will always involve non-spin-flip scattering. The magnetic peaks will involve a mixture of both types of scattering, depending on the orientation of the atomic moments and neutron polarization relative to the scattering vector.

Case I. $\hat{K} \cdot \hat{P}_0 = 1$

Consider first the very useful case in which the neutron polarization is parallel to the scattering vector ($S_{1z} = 0$), as illustrated in Fig. 7(a). The magnetic scattering will be spin-flip and the nuclear scattering will be non-spin-flip. From Eq. (12) the partial cross sections are

$$\frac{d\sigma^{\pm\pm}}{d\Omega} = \sum_{ij} e^{i\mathbf{K} \cdot (\mathbf{r}_i - \mathbf{r}_j)} b_i b_j^* \quad (30)$$

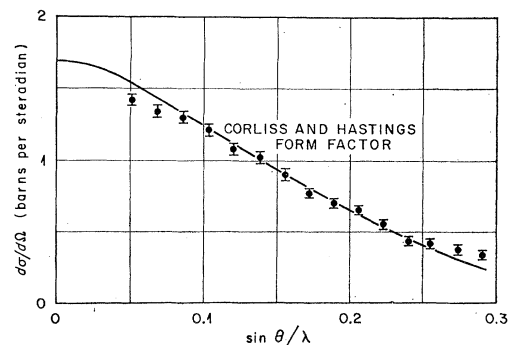


FIG. 6. MnF_2 paramagnetic cross section.

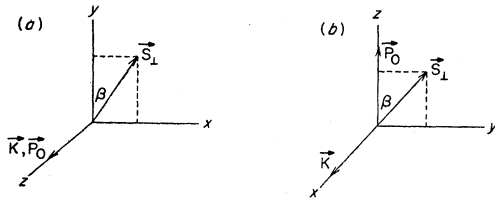


FIG. 7. In (a), $S_{1z}=0$, and S_{1x} and S_{1y} both produce spin-flip scattering. In (b), $S_{1x}=0$, S_{1y} produces spin-flip scattering, and S_{1z} produces non-spin-flip scattering.

and

$$\frac{d\sigma^{\pm\mp}}{d\Omega} = \sum_{ij} e^{i\mathbf{K}\cdot(\mathbf{r}_i-\mathbf{r}_j)} p_i p_j^* [\mathbf{S}_{1i}\cdot\mathbf{S}_{1j} \mp i\hat{z}\cdot(\mathbf{S}_{1i}\times\mathbf{S}_{1j}^*)]. \quad (31)$$

The application to antiferromagnetic structures is obvious—a complete separation of nuclear and magnetic peaks can be obtained at a single temperature. For many antiferromagnets, some of the magnetic peaks will come at the same scattering angle as a nuclear peak. In the usual unpolarized-beam experiment the nuclear peaks are measured at a temperature above the Néel point and then the sample is cooled to well below the Néel point to observe the combined nuclear plus magnetic intensities. The magnetic intensities are then obtained by subtraction. Sometimes this procedure involves large Debye-Waller corrections, or, more seriously, the crystal structure may change at or below the Néel point. An example of isothermal separation of nuclear and magnetic peaks is shown in Fig. 8 for α - Fe_2O_3 powder. The data were collected as in a usual powder scan with the analyzer set for elastic scattering. Note that the aluminum peaks from the sample holder show up only in the nuclear (non-spin-flip) pattern. This technique has recently been used to demonstrate the absence of antiferromagnetism in Ti_2O_3 .²⁰

The experimental configuration with $\hat{\mathbf{K}}\cdot\hat{\mathbf{P}}_0=1$ is not generally useful for Bragg scattering from ferromagnets because this implies that the sample is magnetized along $\hat{\mathbf{K}}$ and then $S_1=0$. However, we have recently used just this arrangement to search for noncollinear spin density in hexagonal Co .²¹ Any component of the spin density normal to the magnetization direction would produce elastic spin-flip scattering. Such scattering was not observed.

Case II. $\mathbf{K}\cdot\mathbf{P}_0=0$

We select a coordinate system as illustrated in Fig. 7(b) so that $S_{1x}=0$. The magnetic scattering will be either spin-flip, non-spin-flip, or a mixture, depending on the orientation of the atomic moments. From Eq.

²⁰ R. M. Moon, T. Riste, W. C. Koehler, and S. C. Abrahams, in Proceedings of the Fourteenth Annual Conference on Magnetism and Magnetic Materials, New York, 1968 (unpublished); J. Appl. Phys. (to be published).

²¹ R. M. Moon and W. C. Koehler, this issue, Phys. Rev. **181**, 883 (1969).

(12) the partial cross sections are

$$\frac{d\sigma^{\pm\pm}}{d\Omega} = \sum_{ij} e^{i\mathbf{K}\cdot(\mathbf{r}_i-\mathbf{r}_j)} [b_i b_j^* \mp (b_i p_j^* S_{1xz}^* + b_j^* p_i S_{1xi}) + p_i p_j^* S_{1xi} S_{1xz}^*], \quad (32)$$

$$\frac{d\sigma^{\pm\mp}}{d\Omega} = \sum_{ij} e^{i\mathbf{K}\cdot(\mathbf{r}_i-\mathbf{r}_j)} p_i p_j^* S_{1xi} S_{1xi}^*. \quad (33)$$

In the non-spin-flip cross section are the familiar terms giving purely nuclear scattering, purely magnetic scattering, and the nuclear-magnetic interference scattering. The atomic-spin components involved are those perpendicular to the scattering vector and parallel to the neutron polarization. The spin-flip scattering is produced by atomic-spin components which are perpendicular to both the scattering vector and the neutron polarization. For collinear ferromagnets, the atomic spins are aligned along the neutron-polarization direction, so that the spin-flip scattering vanishes. Nothing is gained in this case by doing a polarization analysis experiment instead of the usual measurement of the polarization dependence of the total cross section, unless one wishes to search for departures from collinearity.

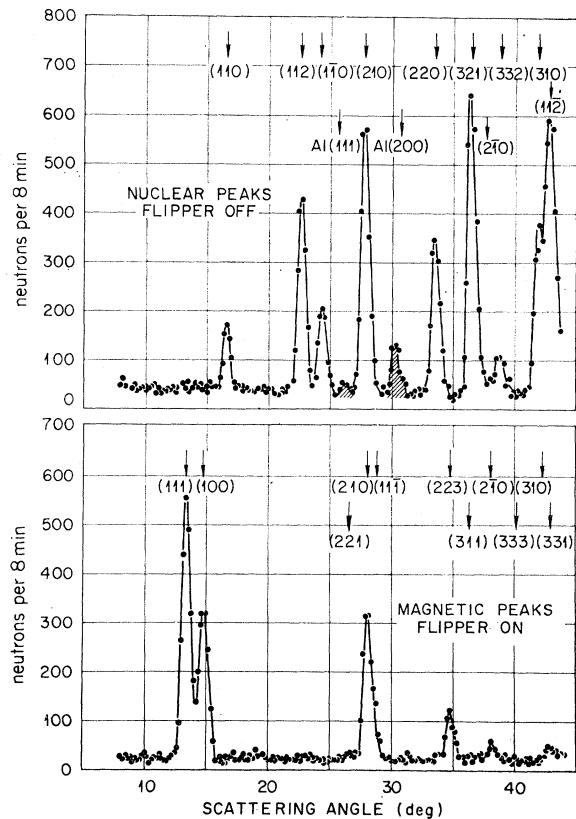


FIG. 8. α - Fe_2O_3 powder pattern—separation of nuclear and magnetic peaks through polarization analysis. $\hat{\mathbf{K}}\cdot\hat{\mathbf{P}}_0=1$.

For an antiferromagnet, the nuclear-magnetic interference terms will usually vanish. The purely magnetic intensity from a single-domain, collinear antiferromagnet should then have the following dependence on β , the angle between \mathbf{S}_1 and \hat{P}_0 :

$$I_{\text{mag}}^{\pm\pm} = I_0 \cos^2\beta, \quad (34)$$

$$I_{\text{mag}}^{\pm\mp} = I_0 \sin^2\beta. \quad (35)$$

Rotating the crystal about the scattering vector should shift the magnetic intensity from non-spin-flip scattering to spin-flip scattering. This would be a useful technique in establishing spin directions^{22,23} and/or domain populations.

Rather than attempt to catalog the variety of effects that can be observed with complicated structures through polarization analysis techniques, we wish to emphasize the basic simplicity of the underlying physics. To predict the effects to be expected from any structure, one has only to remember that components of \mathbf{S}_1 which are perpendicular to the neutron polarization will produce spin-flip scattering, while the component parallel to the neutron polarization will produce non-spin-flip scattering. We believe the technique will have important applications in work on antiferromagnetic structures. Many existing reactors have sufficient flux for polarization analysis of Bragg scattering. In addition, the first and third axes may have fixed scattering angles, so that any existing polarized-beam diffractometer can be readily converted for elastic polarization analysis. It should also be noted that for antiferromagnetic studies, only a modest field of ~ 100 G is necessary at the sample position to guide the neutron polarization.

VI. COHERENT INELASTIC SCATTERING

In this section we will be primarily concerned with the polarization effects in magnon scattering. The coherent nuclear phonon scattering is always non-spin-flip scattering. In an ordered magnetic material there will be additional magnetic inelastic scattering in which phonons are excited through the magnetic interaction. This magnetovibrational scattering is elastic with respect to the spin system and exhibits polarization effects similar to the magnetic Bragg scattering.

The first polarization effect to be studied in spin-wave scattering was the polarization dependence of the cross section. Our primary concern is with the change of polarization accompanying spin-wave scattering and with the creation of polarization when an unpolarized beam is scattered by spin waves. The basic equations for calculating these effects have been given

²² R. Nathans, T. Riste, G. Shirane, and C. G. Shull, *Bull. Am. Phys. Soc.* **2**, 1, FA4 (1957).

²³ S. A. Werner and A. Arrott, in *Proceedings of the Fourteenth Annual Conference on Magnetism and Magnetic Materials*, New York, 1968 (unpublished); *J. Appl. Phys.* (to be published).

by Sáenz,⁴ by Izyumov and Maleev,^{3,5,6} by Steinsvoll,¹¹ and by Lovesey.²⁴ Some experimental studies of the same phenomena have been reported by Drabkin and co-workers.^{25,26} Our present work has been briefly reported earlier.²⁷ Again we assume a system in which the nuclear spins, if present, are randomly oriented, so that we neglect terms involving \mathbf{I} when discussing coherent scattering.

Ferromagnets

In performing polarized-beam experiments on ferromagnets, the sample must be magnetized to saturation to avoid serious depolarization effects. Thus the neutron polarization is always parallel to the magnetization. We write the atomic spin as $\mathbf{S} = S_x \hat{x} + S_y \hat{y}$, where \hat{x} is along the magnetization and neutron-polarization direction. Spin waves are correlations between the S_x and S_y components on different sites. The effective magnon scattering vectors will be $S_x(\hat{x} - (\hat{x} \cdot \hat{K})\hat{K})$, with a similar expression for the y component. For a general orientation of \hat{K} and \hat{x} , these effective magnon scattering vectors will have a component along \hat{x} , giving non-spin-flip scattering, and another component transverse to \hat{x} , giving spin-flip scattering. There are two experimentally important special cases in which the magnon scattering is purely spin-flip and which can be easily analyzed in terms of the amplitude equations (6).

Consider first the case where the polarization, magnetization, and scattering vectors are all collinear ($S_{1z} = 0$, $S_{1x} = S_x$, and $S_{1y} = S_y$). The spin-flip amplitude equations reduce to the familiar step-up and step-down ladder operators. These are the operators required for creation and annihilation of spin waves in a Heisenberg ferromagnet. The ground state of the system is $-\text{NS}$, so the step-up operator, associated with the $(+ -)$ cross section, corresponds to magnon creation and neutron energy loss, and the step-down operator, associated with the $(- +)$ cross section, involves magnon annihilation and neutron energy gain. The total spin of the system plus neutron is conserved. All the interesting effects may now be easily understood. If the neutrons are polarized in the $(+)$ state, only the magnon creation peak will be observed, and if they are in the $(-)$ state, only the annihilation peak will be observed. If the beam is unpolarized (both states equally populated), both peaks will be observed with the creation peak polarized in the $(-)$ direction and the annihilation peak polarized in the $(+)$ direction. We have demonstrated these effects by experiments on $\text{Fe}_{2.5}\text{Li}_{0.5}\text{O}_4$,

²⁴ S. W. Lovesey, Report No. T.P. 351, AERE, Harwell, 1968 (unpublished).

²⁵ G. M. Drabkin, E. I. Zabidarov, Ya. A. Kasman, A. I. Okorokov, and V. A. Trunov, *Zh. Eksperim. i Teor. Fiz.* **47**, 2316 (1964) [English transl.: *Soviet Phys.—JETP* **20**, 1548 (1965)].

²⁶ G. M. Drabkin, E. I. Zabidarov, Ya. A. Kasman, and A. I. Okorokov, *Zh. Eksperim. i Teor. Fiz. Pis'ma v Redaktsiyu* **2**, 541 (1965) [English transl.: *Soviet Phys.—JETP Letters* **2**, 336 (1965)].

²⁷ T. Riste, R. M. Moon, and W. C. Koehler, *Phys. Rev. Letters* **20**, 997 (1968).

lithium ferrite. Low-energy ferrimagnetic spin waves are known to obey a quadratic dispersion law and thus behave like ferromagnetic spin waves. In Fig. 9(a) is shown the reversal of polarization in spin-wave scattering by magnon creation. In this case the flipper was located after the sample so that the peak corresponds to a (+-) cross section. The data were collected by offsetting the crystal through +5° from the (111) Bragg position and then analyzing the scattered neutrons by rotating the analyzer and counter in a θ - 2θ relationship. The creation of polarization in spin-wave scattering has already been reported.²⁷ In this experiment the incident beam was depolarized by inserting an iron shim and the flipper was again located after the sample. Both annihilation and creation peaks were observed, but polarized in opposite directions. The creation peak appeared in the "flipper-on" data and hence is associated with (+-) scattering, and the annihilation peak appeared in the "flipper-off" data and is associated with (-+) scattering. These effects are also demonstrated in Fig. 10, which was obtained by performing a constant \mathbf{K} (or \mathbf{Q}) scan at the (111) position. The positive-energy side corresponds to magnon creation (energy gained by the system). The flipper was located after the sample and the plot gives the difference between counts recorded with the flipper off and with the flipper on. With the incident beam unpolarized we see that both creation and annihilation processes are contributing to the scattering with roughly equal intensities, and with the scattered neutrons polarized oppositely for the two processes. With the incident beam polarized in the (+) state, only (+-) spin-flip scattering is possible. The magnon creation scattering should then double because we have increased the number of incident neutrons in the (+) state by a factor of 2, and the annihilation scattering should fall to zero. Actually, a small intensity remained on the annihilation side because of the rather low polarization ($\sim 90\%$) in this particular experiment.

For the case in which $\hat{\mathbf{K}} \cdot \hat{\mathbf{P}}_0 = 0$, we can select a coordinate system where the y axis is along the scattering

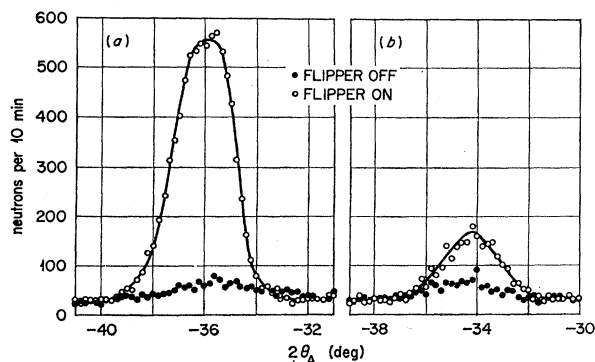


FIG. 9. Polarization reversal in magnon scattering from Li ferrite. In (a), $\hat{\mathbf{K}} \cdot \hat{\mathbf{P}}_0 = 1$, and in (b), $\hat{\mathbf{K}} \cdot \hat{\mathbf{P}}_0 = 0$. The small peak in the flipper-off data is due to nuclear disorder scattering.

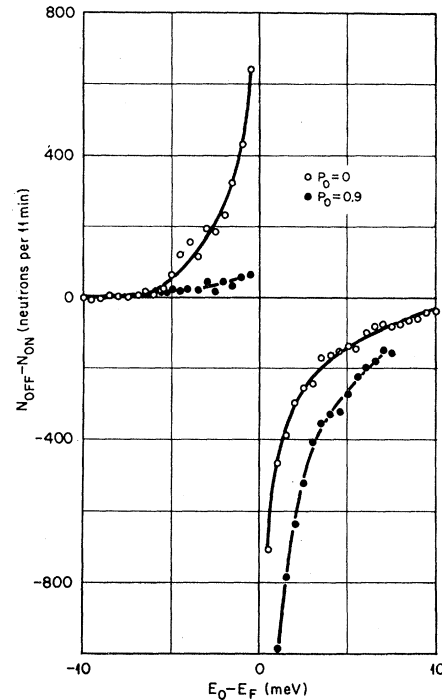


FIG. 10. Flipper-off-flipper-on intensity in constant- Q scan at (111) position in Li ferrite. $\hat{\mathbf{K}} \cdot \hat{\mathbf{P}}_0 = 1$. Imperfect instrumental resolution allows the observation of low- q magnon scattering for both creation and annihilation processes.

vector; hence $S_{1y} = 0$ and $S_{1x} = S_x$. In this case we have only $S_x S_x$ -type correlations contributing to the spin-wave scattering. If we write $S_x = \frac{1}{2}(S^+ + S^-)$, where the + and - refer to the step-up and step-down operators, the spin-flip amplitudes become

$$U^{+-} = U^{-+} = -\frac{1}{2}p(S^+ + S^-), \quad (36)$$

so that both spin-flip processes contribute to both creation and annihilation peaks. If the initial beam is polarized, we expect both creation and annihilation peaks, each with $\frac{1}{4}$ the intensity of the single peak appearing in the case $\hat{\mathbf{K}} \cdot \hat{\mathbf{P}}_0 = 1$. This is illustrated in Fig. 9(b). For this experiment the flipper was located before the sample and the crystal was offset -5° from the Bragg position, so that we are observing a (+-) scattering process associated with magnon annihilation. If the initial beam is unpolarized, both (+-) and (-+) processes will contribute equally to both peaks, so we expect the scattered neutrons to have zero polarization. This is illustrated in Fig. 11. The absence of polarization in this case is also predicted by Eq. (20). The term $(\hat{\mathbf{A}}_i \times \hat{\mathbf{A}}_j^*)$ describes the polarization created in spin-wave scattering, so that it is the $S_{1x} S_{1y}$ -type correlations that are important. In the geometry we are now considering, $S_{1y} = 0$, so that there is no polarization created.

All of the above observations are correctly described by the following general formulas for scattering by spin waves in a Heisenberg ferromagnet. The final polar-

ization was first derived by Izyumov and Maleev,⁵

$$P = \frac{\mp 2\hat{K}(\hat{K} \cdot \hat{m}) - \mathbf{P}_0[1 + (\hat{K} \cdot \hat{m})^2] + 2\mathbf{M}_x(\mathbf{M}_x \cdot \mathbf{P}_0) + 2\mathbf{M}_y(\mathbf{M}_y \cdot \mathbf{P}_0)}{1 + (\hat{K} \cdot \hat{m})^2 \pm 2(\mathbf{P}_0 \cdot \hat{K})(\hat{K} \cdot \hat{m})}, \quad (37)$$

and the total cross section was first given by Sáenz,⁴

$$\frac{d\sigma}{d\Omega} \sim [1 + (\hat{K} \cdot \hat{m})^2 \pm 2(\mathbf{P}_0 \cdot \hat{K})(\hat{m} \cdot \hat{K})]. \quad (38)$$

The upper sign refers to the creation of spin waves and the lower sign to annihilation, and \hat{m} is a unit vector in the direction of the magnetization. The vector $\mathbf{M}_x = \hat{x} - (\hat{x} \cdot \hat{K})\hat{K}$, with a similar definition for \mathbf{M}_y , where \hat{x} and \hat{y} are both orthogonal to \hat{m} . Actually, Eq. (38) goes all the way back to Halpern and Johnson, who derived a similar cross section for the case of scattering in a ferromagnet where a single ion decreases its spin by unity. We expect (37) and (38) to apply to collective excitation (spin waves) and to single-particle excitations (Stoner modes).

It is worth noting that all of the discussion in this section strictly applies only to the case of a Heisenberg ferromagnet. In particular, for the case where $\hat{K} \cdot \hat{m} = 1$, the vanishing of the cross section for magnon annihilation with a polarized beam ($P_0 = +1$) and the creation of complete polarization in the magnon peaks for an unpolarized beam follow from the fact that the operators appearing in the spin-flip amplitude equations

[when substituted in Eq. (2)] are just those needed for creation and annihilation of magnons in a Heisenberg ferromagnet. This will not be the case for a different Hamiltonian, and Samuelson²⁸ has suggested that experiments such as those described above may provide a sensitive test for the validity of the Heisenberg Hamiltonian, and may also provide information on the nature of the true Hamiltonian.

Antiferromagnets

The major experimental difference between this case and the ferromagnetic case is that with antiferromagnets the neutron polarization and the sublattice magnetization need not be in the same direction. Therefore the spin components involved with spin waves are not necessarily transverse to the neutron polarization. Hence the polarization of the scattered neutrons may be unchanged, partly reversed, or completely reversed, depending on the experimental conditions.

We have demonstrated this by experiments on α -Fe₂O₃. At room temperature the spins are in the rhombohedral (111) plane, the basal plane. In the absence of an external field there is no single preferred spin direction in this plane. However, in a field of about 5 kOe in the basal plane, the domain population is altered so that all the spins are perpendicular to the field. This has been demonstrated by polarization analysis of Bragg-scattered neutrons.²² Figure 12 shows the results of polarization analysis of low-energy (~ 5 -meV) magnons near the (111) position. In Fig. 12(a) the field is applied vertically in the (111) plane, and is strong enough to induce a unique horizontal antiferromagnetic axis. Referring to the amplitude equations (6), we select the coordinate system so that $S_{1z} = 0$. The spins will then be very close to the y axis and the spin-wave scattering will be produced by correlations in the z components. The spin-wave scattering should then be non-spin-flip, as is observed. In Fig. 12(b), a weak field is applied in the same direction, sufficient to maintain the neutron polarization in the vertical direction, but low enough to give an approximately random alignment of the spins in the (111) plane. There are then approximately equal contributions to the spin-wave scattering by y (spin-flip) and z (non-spin-flip) components, so that the final polarization should be zero. The small deviation from this value shown by the data is due to some degree of spin alignment caused by the nonzero field. In Fig. 12(c) the initial polarization

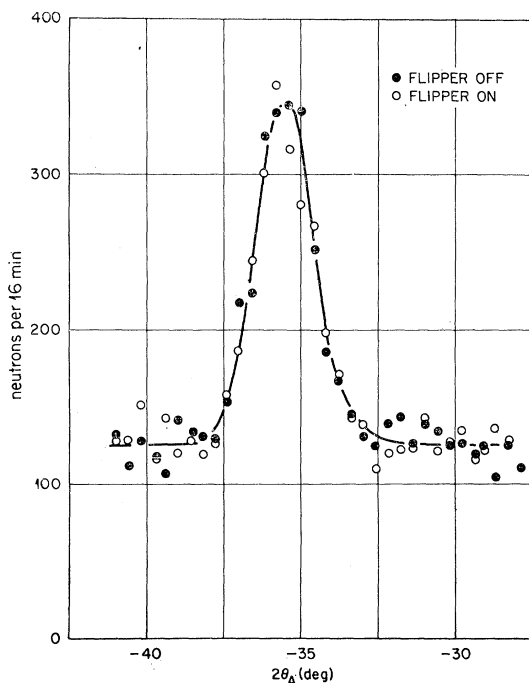


FIG. 11. Absence of polarization in magnon scattering from Li ferrite with $\hat{K} \cdot \hat{P}_0 = 0$. The incident beam was unpolarized and the flipper was after the sample.

²⁸ E. J. Samuelson (private communication).

is along the scattering vector ($S_{1z}=0$) and only spin-flip scattering is observed.

The final polarization of neutrons scattered by antiferromagnetic spin waves in the Heisenberg model is in agreement with the following formula given by Izyumov and Maleev⁵:

$$P = 2 \frac{\mathbf{P}_0' - \hat{K}'(\mathbf{P}_0 \cdot \hat{K}) + \hat{K}(\hat{K} \cdot \hat{m})(\mathbf{M} \cdot \hat{P}_0)}{1 + (\hat{K} \cdot \hat{m})^2} - \mathbf{P}_0, \quad (39)$$

where the prime suffix denotes the component transverse to the unit sublattice magnetization vector \hat{m} , and $\mathbf{M} = \hat{m} - (\hat{m} \cdot \hat{K})\hat{K}$.

These demonstration experiments on $\text{Fe}_{2.5}\text{Li}_{0.5}\text{O}_4$ and $\alpha\text{-Fe}_2\text{O}_3$ were performed under conditions known to give the possibility of observing spin-wave scattering undisturbed by other intensity components. However, we expect the polarization analysis technique to prove useful in distinguishing between nuclear phonon scattering, magnetovibrational scattering, and magnon scattering. In a ferromagnet the same distinction may be obtained by using the polarization dependence of the total cross section, as demonstrated by Steinsvoll.²⁹ However, it may be more convenient, and better in terms of neutron economy, to use an unpolarized beam with polarization analysis of the scattered neutrons. The bulk of the dispersion curve data could then be collected with highly reflecting, nonpolarizing crystals at both the monochromator and analyzer positions. Those cases where the identity of a peak is ambiguous could be investigated by replacing the analyzer with a polarization-sensitive crystal. If the sample is magnetized along the scattering vector, the magnetovibrational intensity should vanish, the final polarization of a phonon peak should be zero, and that of a magnon peak should be ± 1 . As in the case of Bragg scattering, the real advantage of polarization analysis for inelastic coherent scattering comes in applications to the study of antiferromagnets. This is the only technique for separating magnon and phonon scattering for systems in which the direction of the atomic spins cannot be controlled. With the neutron polarization along the scattering vector, the non-spin-flip scattering will be nuclear phonon scattering, and the spin-flip scattering will be the sum of magnetic phonon scattering (magnetovibrational) and magnon scattering. Since the ratio of magnetic to nuclear phonon scattering is the same as in the Bragg peak around which the inelastic scattering is observed (correcting for the magnetic form-factor dependence), it should be possible to separate the three cross sections completely by doing

²⁹ O. Steinsvoll, in *Neutron Inelastic Scattering* (International Atomic Energy Agency, Vienna, 1968), Vol. II.

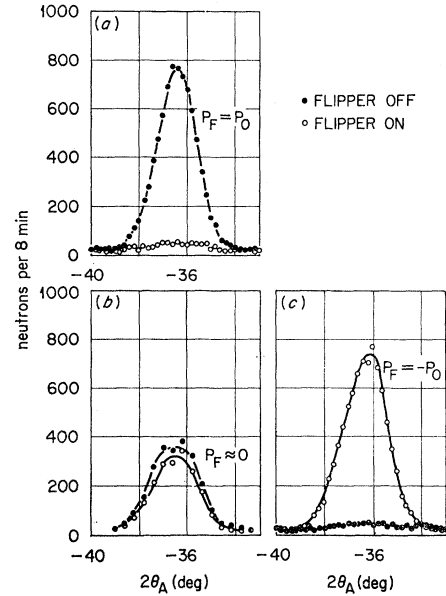


FIG. 12. Polarization analysis of spin-wave scattering by magnon creation in $\alpha\text{-Fe}_2\text{O}_3$, $\Delta\theta = +10^\circ$ from (111). For (a), $\hat{K} \cdot \hat{P}_0 = 0$, $H = 9$ kOe. For (b), $\hat{K} \cdot \hat{P}_0 = 0$, $H \approx 0$. For (c), $\hat{K} \cdot \hat{P}_0 = 1$.

polarization analysis experiments on both the Bragg peak and the inelastic peak.

VII. SUMMARY

Polarization analysis is a versatile tool for identifying spin-dependent scattering processes. In analyzing experimental results, or in planning new experiments, it is helpful, and almost sufficient, to remember that components of the effective spin [defined in Eq. (7)] which are parallel to the neutron polarization produce non-spin-flip scattering, while those perpendicular to the neutron polarization produce spin-flip scattering.

The areas of useful application of this technique include (a) separation of nuclear and magnetic Bragg scattering from antiferromagnets, (b) separation of magnon and phonon scattering from ferromagnets and antiferromagnets, (c) separation of paramagnetic scattering from other types of incoherent scattering, and (d) separation of coherent and spin-incoherent nuclear scattering in solids and liquids. Unfortunately, serious intensity difficulties limit the present application of this technique. At many existing reactors, the technique could be employed for structural studies of antiferromagnets. With the development of polarizing crystals of higher reflectivity, and with the advent of higher-flux reactors, many more areas of research should be open to this technique.